cell with four flat and four pointed rhombohedra, and model II has a complicated unit cell involving 32 flat and 52 pointed rhombohedra, plus rules for accommodating modulations. Model II bears an obvious resemblance to the aperiodic structures attempted by others (*e.g.* Levine & Steinhardt, 1984). In view of the success of model I in leading to the derivation of additional periodicities through sublattices, and in explaining the possibility of observing icosahedral diffraction patterns, it is preferred for its physical plausibility over either the model II unit cell or the undecorated aperiodic structures.

In conclusion, the electron diffraction patterns taken from icosahedral phase Al-Mn can be understood in terms of an icosahedral cubic reference lattice derived from six modulation vectors $\mathbf{q}_i^{(1)}$ plus six collinear modulations $\mathbf{q}_i^{(2)}$. The appearance of the six $\mathbf{r}_i$'s may be taken together with theoretical results of Bak (1985). However, if the model derived in this work is to be understood within the context of ordinary incommensurate modulated crystals, the theory would have to be generalized to include structures for which the observed point symmetry is already realized in the unit cell of the reference lattice. Naturally, the pattern of atomic sites in this derived unit cell of the reference lattice is excluded from the 230 space groups because it conforms to icosahedral point symmetry.

In retrospect, once the experimental data required six independent vectors for indexing the diffraction pattern and for the construction of an atomic motif, the appearance of more than one three-dimensional periodicity was inevitable. In the following paper (Kuriyama & Long, 1986) the full mathematical structures of the **a** cell and the $\mathbf{a}^+$ sublattices are given. It is also shown how they are accommodated into a structure consistent with both sets of modulation vectors. In that work the full structure factor in terms of atomic positions is derived.

The authors gratefully acknowledge assistance with the experiment by L. Bendersky. We are also indebted to H. Fowler for his calculations in the preparation of Figs. 5 and 6, and to R. Roth for useful discussions.

References

BAK, P. (1985). *Phys. Rev. Lett.* **54**, 1517-1519.

BOETTINGER, W. J. (1984). Private communication.

COWLEY, J. W. (1981). *Diffraction Physics*, 2nd ed. Amsterdam: North Holland.

DEHLINGER, U. (1928). *Kristallografiya*, **65**, 615-631.

FONTAINE, D. DE (1966). *Local Atomic Arrangements Studied by X-ray Diffraction*, edited by J. B. COHEN & J. E. HILLIARD, pp. 51-94. New York: Gordon & Breach.

FUJIMOTO, F. (1959). *J. Phys. Soc. Jpn*, **14**, 1558-1568.

FUJIWARA, K. (1957). *J. Phys. Soc. Jpn*, **12**, 7-13.

HOGGATT, V. E. (1969). *Fibonacci and Lucas Numbers*. Boston: Houghton Mifflin.

KITTEL, C. (1976). *Introductioin to Solid State Physics*, 5th ed., p. 9. New York: John Wiley.

KRAMER, P. & NERI, R. (1984). *Acta Cryst.* A**40**, 580-587.

KURIYAMA, M. (1970). *Acta Cryst.* A**26**, 56-59.

KURIYAMA, M. (1975). *Acta Cryst.* A**31**, 774-779.

KURIYAMA, M. & LONG, G. G. (1986). *Acta Cryst.* A**42**, 164-172.

KURIYAMA, M., LONG, G. G. & BENDERSKY, L. (1985). *Phys. Rev. Lett.* **55**, 849-851.

KURIYAMA, M. & MIYAKAWA, T. (1969). *J. Appl. Phys.* **40**, 1697-1702.

LAUE, M. VON (1912). *Proc. Bav. Acad. Sci.* pp. 303-312, 363-372.

LEVINE, D. & STEINHARDT, P. J. (1984). *Phys. Rev. Lett.* **53**, 2477-2480.

MACKAY, A. L. (1981). *Sov. Phys. Crystallogr.* **26**, 517-522.

MACKAY, A. L. (1982). *Physica (Utrecht)*, **114**A, 609-613.

NELSON, D. R. & SACHDEV, S. (1985). *Phys. Rev. B*, **32**, 689-695.

NICOL, A. D. I. (1953). *Acta Cryst.* **6**, 285-293.

NIEHRS, H. (1959). *Z. Naturforsch. Teil A*, **14**, 504-511.

PENROSE, R. (1974). *J. Inst. Math. Its Appl.* **10**, 266-271.

SHECHTMAN, D., BLECH, I., GRATIAS, D. & CAHN, J. W. (1984). *Phys. Rev. Lett.* **53**, 1951-1953. [See also *Phys. Today*, (1985), **38**, 17-19.]

STURKEY, L. (1957). *Acta Cryst.* **10**, 858.

Acta Cryst. (1986). A**42**, 164-172

Single-Crystal Structure of Rapidly Cooled Alloys with Icosahedral Symmetry. II. Theoretical Analysis – Internal Modulations

BY MASAO KURIYAMA AND GABRIELLE GIBBS LONG

Institute for Materials Science and Engineering, National Bureau of Standards, Gaithersburg, MD 20899, *USA*

(*Received* 14 *August* 1985; *accepted* 4 *November* 1985)

Abstract

The icosahedral cubic cell, derived in the first of this set of two papers, is further developed. Rules for the occupancy of atomic sites are derived based on periodic modulations over the reference lattice. The form of the derived structure, which involves partial Fibonacci sequence stacking, suggests that the true structure is the limit of a superposition of successively larger periodic sequences. The structure factor for the limiting (nonperiodic) structure is derived and some physical insights into the application of almost periodic functions to icosahedral phase Al-Mn are given.

1. Introduction

This is the second in a series of two papers on the atomic scale structure of icosahedral phase Al–Mn alloys. In the first paper (Long & Kuriyama, 1986), hereinafter called I (see also Kuriyama, Long & Bendersky, 1985), a unit cell for a reference cubic lattice was derived which was called 'icosahedral cubic'. The approach of these papers (both I and II) has been to explore the unique opportunity offered by the fabrication of an icosahedral phase alloy.

In I, the electron diffraction patterns taken from this material resulted in the identification of two colinear sets of six modulation vectors in momentum space. After conversion to real space, one set was considered to be 'correlation distances'. Using these, an atomic arrangement was found which led to the identification of a unit cell of the reference lattice. The two rhombohedra commonly used in nonperiodic icosahedral models were derived, where these rhombohedra are decorated by atomic sites on each face as well as at each vertex.

Although the unit cell in I conforms to the icosahedral point group, it alone cannot account for the diffraction patterns. Either there is another three-dimensional periodicity or lattice(s), or the second set of modulations is a physical phenomenon. Since each diffraction spot was indexed by six (modulation) vectors and only three vectors define the unit cell, three more vectors in real space were sought. This would produce a structure in which sublattices coexist with the reference lattice. Another way of deriving the full atomic scale structure (and understanding the diffraction patterns) would be to accept the second set of six modulation vectors as physical modulations of the structure. In this case, as in the case above, the sublattice sites are derived. Thus, these two approaches are closely related. In either case, our understanding of modulated structures would have to be generalized.

In contrast to the phenomenological treatment of the diffraction patterns, the objective of this series of papers is to identify the atomic structure for this material. The experimental analysis in I is in agreement with the vertex model (Nelson & Sachdev 1985). However, that model alone is inadequate for the determination of an atomic structure.

In this work, the properties of the unit cell are studied and the rules for packing and occupancy of atomic sites are developed. In § 2, the correlation vectors for the framework of the model are given and it is shown that the transformation matrix relating one possible reference unit cell in the model to another is the icosahedral transformation. The atomic sites associated with the reference lattice, which were used in I, are given explicitly in § 3, and are used to derive other atomic sites consistent with the model. In § 4, rules for the occupancy of atomic sites are developed through staggered layering based on periodic modulations over the reference lattice. Finally, the limit of the staggered occupancy sequence is taken for successively larger periodic modulations. This yields the staggering sequence as the superposition of all these periodic modulations. The Fourier transform for this limiting system is given in § 5.

Table 1. *Observed modulations in momentum space*

$$\mathbf{q}_1 = q \sin\theta\,(\tau, 1, 0)$$
$$\mathbf{q}_2 = q \sin\theta\,(1, 0, \tau)$$
$$\mathbf{q}_3 = q \sin\theta\,(0, \tau, 1)$$
$$\mathbf{q}_4 = q \sin\theta\,(-1, 0, \tau)$$
$$\mathbf{q}_5 = q \sin\theta\,(0, \tau, -1)$$
$$\mathbf{q}_6 = q \sin\theta\,(\tau, -1, 0)$$

2. Correlation vectors

The good agreement between the calculated diffraction patterns and the experimental patterns in I demonstrates that the positions of the diffraction spots are given by $\sum n_i \mathbf{q}_i$, where $i = 1, \ldots, 6$ and the $\mathbf{q}_i$'s are given in Table 1. (Since the two sets of modulation vectors are colinear, only one set of six vectors is used in what follows.) The modulation vectors in this table are described using a Cartesian coordinate system, *Oxyz*, in which the z axis is [001] perpendicular to a twofold diffraction pattern, and x and y are two other twofold axes, [100] and [010], respectively. The value of τ is given by $\cos\theta/\sin\theta$, where the experimental data demonstrate that the angle θ is the icosahedral angle ($=31.717\ldots°$). Then τ is the Golden Section and is equal to $(1+\sqrt{5})/2$.

In all of the electron diffraction patterns one can recognize periodic repetitions of the positions of diffraction spots. This is true of the three- and fivefold

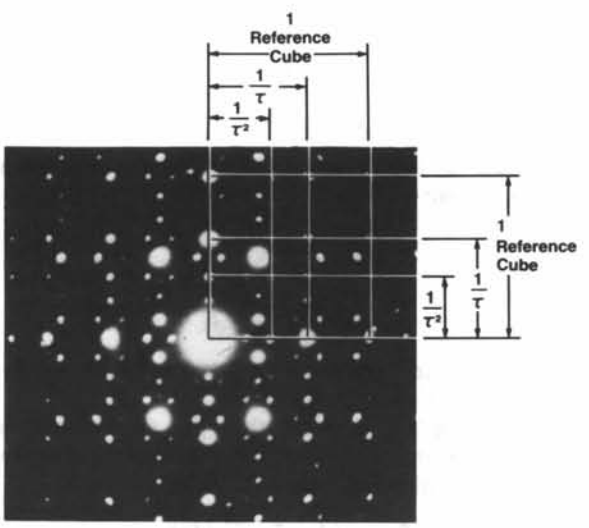

Fig. 1. Three possible reference frames superimposed on a twofold pattern. The frame labeled 1 was assumed to be a reference lattice in paper I.

Table 2. *A preliminary choice of the two reference lattices*

$$\mathbf{a}_1^+ = 1/q \sin 2\theta\,(\sin\theta, 0, 0)$$
$$\mathbf{a}_2^+ = 1/q \sin 2\theta\,(0, \sin\theta, 0)$$
$$\mathbf{a}_3^+ = 1/q \sin 2\theta\,(0, 0, \sin\theta)$$
$$\mathbf{a}_1 = 1/q \sin 2\theta\,(\cos\theta, 0, 0)$$
$$\mathbf{a}_2 = 1/q \sin 2\theta\,(0, \cos\theta, 0)$$
$$\mathbf{a}_3 = 1/q \sin 2\theta\,(0, 0, \cos\theta)$$

$\mathbf{a}_i^+$'s and $\mathbf{a}_i$'s correspond to $\mathbf{a}_i^+$(III)'s and $\mathbf{a}_i$(III)'s, respectively, in Tables 4 and 5 which follow.

patterns, as well as the twofold (paper I). In the twofold pattern, three square frames are easily seen (Fig. 1). The largest frame was originally selected to be the reference reciprocal lattice. It was later found that the reference frames themselves could be created as sums and differences of pairs of $\mathbf{q}_i$'s. For example, the largest reciprocal-lattice frame could be obtained by $\mathbf{b}_1^+ = \mathbf{q}_1 + \mathbf{q}_6$, $\mathbf{b}_2^+ = \mathbf{q}_3 + \mathbf{q}_5$ and $\mathbf{b}_3^+ = \mathbf{q}_2 + \mathbf{q}_4$ and the middle frame by $\mathbf{b}_1 = \mathbf{q}_2 - \mathbf{q}_4$, $\mathbf{b}_2 = \mathbf{q}_1 - \mathbf{q}_6$ and $\mathbf{b}_3 = \mathbf{q}_3 - \mathbf{q}_5$. From these frames in reciprocal space, one can obtain the reference frames, $\mathbf{a}_i$ and $\mathbf{a}_i^+$, in real space given in Table 2.

Next, we define a set of vectors $\mathbf{r}_i$:

$$\begin{pmatrix}\mathbf{r}_1\\ \mathbf{r}_2\\ \mathbf{r}_3\\ \mathbf{r}_4\\ \mathbf{r}_5\\ \mathbf{r}_6\end{pmatrix} = (1/2)\begin{pmatrix}1&0&0&0&1&0\\ 0&0&1&1&0&0\\ 0&1&0&0&0&1\\ 0&0&1&-1&0&0\\ 0&1&0&0&0&-1\\ 1&0&0&0&-1&0\end{pmatrix}\begin{pmatrix}\mathbf{a}_1\\ \mathbf{a}_2\\ \mathbf{a}_3\\ \mathbf{a}_1^+\\ \mathbf{a}_2^+\\ \mathbf{a}_3^+\end{pmatrix} \tag{2.1}$$

or

$$\begin{pmatrix}\mathbf{a}_1\\ \mathbf{a}_2\\ \mathbf{a}_3\\ \mathbf{a}_1^+\\ \mathbf{a}_2^+\\ \mathbf{a}_3^+\end{pmatrix} = \begin{pmatrix}1&0&0&0&0&1\\ 0&0&1&0&1&0\\ 0&1&0&1&0&0\\ 0&1&0&-1&0&0\\ 1&0&0&0&0&-1\\ 0&0&1&0&-1&0\end{pmatrix}\begin{pmatrix}\mathbf{r}_1\\ \mathbf{r}_2\\ \mathbf{r}_3\\ \mathbf{r}_4\\ \mathbf{r}_5\\ \mathbf{r}_6\end{pmatrix}. \tag{2.2}$$

The vectors $\mathbf{r}_i$ are listed in Cartesian coordinates in Table 3, where

$$|\mathbf{r}_i| = r,\ |\mathbf{q}_i| = q, \tag{2.3}$$

and

$$r = (1/2q \sin 2\theta).$$

Then the lattice parameters are $a = |\mathbf{a}_i| = 2\tau r \sin\theta = 2r\cos\theta$ and $a^+ = |\mathbf{a}_i^+| = 2r \sin\theta$.

Since the $\mathbf{q}_i$'s (and thus the $\mathbf{r}_i$'s) are defined in three-dimensional space in terms of the icosahedral angle θ, the following relations hold:

$$\begin{pmatrix}\mathbf{r}_1\\ \mathbf{r}_2\\ \mathbf{r}_3\end{pmatrix} = \begin{pmatrix}1&\tau&\tau\\ \tau&1&\tau\\ \tau&\tau&1\end{pmatrix}\begin{pmatrix}\mathbf{r}_4\\ \mathbf{r}_5\\ \mathbf{r}_6\end{pmatrix}, \tag{2.4}$$

Table 3. *Atomic correlations*

$$\mathbf{r}_1 = r\sin\theta\,(\tau, 1, 0)$$
$$\mathbf{r}_2 = r\sin\theta\,(1, 0, \tau)$$
$$\mathbf{r}_3 = r\sin\theta\,(0, \tau, 1)$$
$$\mathbf{r}_4 = r\sin\theta\,(-1, 0, \tau)$$
$$\mathbf{r}_5 = r\sin\theta\,(0, \tau, -1)$$
$$\mathbf{r}_6 = r\sin\theta\,(\tau, -1, 0)$$

or

$$\begin{pmatrix}\mathbf{r}_4\\ \mathbf{r}_5\\ \mathbf{r}_6\end{pmatrix} = \begin{pmatrix}-1&\tau-1&\tau-1\\ \tau-1&-1&\tau-1\\ \tau-1&\tau-1&-1\end{pmatrix}\begin{pmatrix}\mathbf{r}_1\\ \mathbf{r}_2\\ \mathbf{r}_3\end{pmatrix}, \tag{2.5}$$

where $\tau - 1$ is $1/\tau$.

From (2.1) and (2.2), it is evident that the original choice of sums and differences of pairs of $\mathbf{r}_i$'s is not unique. Another $\mathbf{a}_i$ and $\mathbf{a}_i^+$ set with the same magnitudes could just as consistently have been derived from a permuted set of sums and differences. In all, there are five equivalent sets of reference lattice vectors as listed in Tables 4 and 5. The transformation matrix M relating the reference lattices to each other is the icosahedral transformation

$$\mathsf{M} = (1/2)\begin{pmatrix}1&\tau-1&\tau\\ \tau-1&\tau&-1\\ -\tau&1&\tau-1\end{pmatrix}, \tag{2.6}$$

and $\mathsf{M}^5 = \mathsf{I}$. It turns out that the original examples of $\mathbf{a}_i$ and $\mathbf{a}_i^+$ are the $\mathbf{a}_i$(III) and $\mathbf{a}_i^+$(III) in the tables. Useful relations for generating Tables 4 and 5 are

$$\begin{pmatrix}\mathbf{r}_1\\ \mathbf{r}_2\\ \mathbf{r}_3\end{pmatrix} = (1/2)\begin{pmatrix}\tau-1&1&0\\ 1&0&\tau-1\\ 0&\tau-1&1\end{pmatrix}\begin{pmatrix}\mathbf{a}_1(\mathrm{I})\\ \mathbf{a}_2(\mathrm{I})\\ \mathbf{a}_3(\mathrm{I})\end{pmatrix} \tag{2.7}$$

or

$$\begin{pmatrix}\mathbf{r}_4\\ \mathbf{r}_5\\ \mathbf{r}_6\end{pmatrix} = (1/2)\begin{pmatrix}0&-(\tau-1)&1\\ -(\tau-1)&1&0\\ 1&0&-(\tau-1)\end{pmatrix}\begin{pmatrix}\mathbf{a}_1(\mathrm{I})\\ \mathbf{a}_2(\mathrm{I})\\ \mathbf{a}_3(\mathrm{I})\end{pmatrix}. \tag{2.8}$$

Only the $\mathbf{q}_i^{(1)}$'s lead to a set of $\mathbf{r}_i$'s, which can be considered to be atomic correlation distances. Hereafter it is understood that $\mathbf{a}_i$ $\mathbf{a}_i^+$ and $\mathbf{r}_i$ are all referred to set $\mathbf{q}_i^{(1)}$. As seen in I, the vector set of $\mathbf{a}_i$ *does* serve as the reference lattice. Whether the set of $\mathbf{a}_i^+$ is another reference lattice, or the modulation set $\mathbf{q}_i^{(2)}$ is more fundamental than the $\mathbf{a}_i^+$ lattice(s) will be answered in the following sections.

3. Atomic sites

The atomic sites in this material were found in I to be given by

$$\mathbf{R}(\mathsf{n}) = \sum_{i=1,\ldots,6} n_i \mathbf{r}_i, \tag{3.1}$$

Table 4. *Equivalent choices of the large reference lattice*

I:	$\mathbf{a}_1(\mathrm{I})=\mathbf{r}_2+\mathbf{r}_6$ $\mathbf{a}_2(\mathrm{I})=\mathbf{r}_1+\mathbf{r}_5$ $\mathbf{a}_3(\mathrm{I})=\mathbf{r}_3+\mathbf{r}_4$	$\begin{pmatrix}\mathbf{a}_1(\mathrm{I})\\ \mathbf{a}_2(\mathrm{I})\\ \mathbf{a}_3(\mathrm{I})\end{pmatrix}=\mathsf{M}^5\begin{pmatrix}\mathbf{a}_1(\mathrm{I})\\ \mathbf{a}_2(\mathrm{I})\\ \mathbf{a}_3(\mathrm{I})\end{pmatrix}$
II:	$\mathbf{a}_1(\mathrm{II})=\mathbf{r}_2+\mathbf{r}_3$ $\mathbf{a}_2(\mathrm{II})=\mathbf{r}_1-\mathbf{r}_4$ $\mathbf{a}_3(\mathrm{II})=\mathbf{r}_5-\mathbf{r}_6$	$\begin{pmatrix}\mathbf{a}_1(\mathrm{II})\\ \mathbf{a}_2(\mathrm{II})\\ \mathbf{a}_3(\mathrm{II})\end{pmatrix}=\mathsf{M}\begin{pmatrix}\mathbf{a}_1(\mathrm{I})\\ \mathbf{a}_2(\mathrm{I})\\ \mathbf{a}_3(\mathrm{I})\end{pmatrix}$
III:	$\mathbf{a}_1(\mathrm{III})=\mathbf{r}_3+\mathbf{r}_5$ $\mathbf{a}_2(\mathrm{III})=\mathbf{r}_1+\mathbf{r}_6$ $\mathbf{a}_3(\mathrm{III})=-\mathbf{r}_2-\mathbf{r}_4$	$\begin{pmatrix}\mathbf{a}_1(\mathrm{III})\\ \mathbf{a}_2(\mathrm{III})\\ \mathbf{a}_3(\mathrm{III})\end{pmatrix}=\mathsf{M}^2\begin{pmatrix}\mathbf{a}_1(\mathrm{I})\\ \mathbf{a}_2(\mathrm{I})\\ \mathbf{a}_3(\mathrm{I})\end{pmatrix}$
IV:	$\mathbf{a}_1(\mathrm{IV})=\mathbf{r}_4-\mathbf{r}_5$ $\mathbf{a}_2(\mathrm{IV})=-\mathbf{r}_1-\mathbf{r}_2$ $\mathbf{a}_3(\mathrm{IV})=\mathbf{r}_3-\mathbf{r}_6$	$\begin{pmatrix}\mathbf{a}_1(\mathrm{IV})\\ \mathbf{a}_2(\mathrm{IV})\\ \mathbf{a}_3(\mathrm{IV})\end{pmatrix}=\mathsf{M}^3\begin{pmatrix}\mathbf{a}_1(\mathrm{I})\\ \mathbf{a}_2(\mathrm{I})\\ \mathbf{a}_3(\mathrm{I})\end{pmatrix}$
V:	$\mathbf{a}_1(\mathrm{V})=\mathbf{r}_4-\mathbf{r}_6$ $\mathbf{a}_2(\mathrm{V})=-\mathbf{r}_1-\mathbf{r}_3$ $\mathbf{a}_3(\mathrm{V})=-\mathbf{r}_2-\mathbf{r}_5$	$\begin{pmatrix}\mathbf{a}_1(\mathrm{V})\\ \mathbf{a}_2(\mathrm{V})\\ \mathbf{a}_3(\mathrm{V})\end{pmatrix}=\mathsf{M}^4\begin{pmatrix}\mathbf{a}_1(\mathrm{I})\\ \mathbf{a}_2(\mathrm{I})\\ \mathbf{a}_3(\mathrm{I})\end{pmatrix}$

Table 5. *Equivalent choices of the small reference lattice*

I:	$\mathbf{a}_1^+(\mathrm{I})=\mathbf{r}_1-\mathbf{r}_5$ $\mathbf{a}_2^+(\mathrm{I})=\mathbf{r}_3-\mathbf{r}_4$ $\mathbf{a}_3^+(\mathrm{I})=\mathbf{r}_2-\mathbf{r}_6$	$\begin{pmatrix}\mathbf{a}_1^+(\mathrm{I})\\ \mathbf{a}_2^+(\mathrm{I})\\ \mathbf{a}_3^+(\mathrm{I})\end{pmatrix}=\frac{1}{\tau}\mathsf{I}\begin{pmatrix}\mathbf{a}_1(\mathrm{I})\\ \mathbf{a}_2(\mathrm{I})\\ \mathbf{a}_3(\mathrm{I})\end{pmatrix}$
II:	$\mathbf{a}_1^+(\mathrm{II})=\mathbf{r}_1+\mathbf{r}_4$ $\mathbf{a}_2^+(\mathrm{II})=\mathbf{r}_5+\mathbf{r}_6$ $\mathbf{a}_3^+(\mathrm{II})=-\mathbf{r}_2+\mathbf{r}_3$	$\begin{pmatrix}\mathbf{a}_1^+(\mathrm{II})\\ \mathbf{a}_2^+(\mathrm{II})\\ \mathbf{a}_3^+(\mathrm{II})\end{pmatrix}=\frac{1}{\tau}\mathsf{M}\begin{pmatrix}\mathbf{a}_1(\mathrm{I})\\ \mathbf{a}_2(\mathrm{I})\\ \mathbf{a}_3(\mathrm{I})\end{pmatrix}$
III:	$\mathbf{a}_1^+(\mathrm{III})=\mathbf{r}_1-\mathbf{r}_6$ $\mathbf{a}_2^+(\mathrm{III})=\mathbf{r}_2-\mathbf{r}_4$ $\mathbf{a}_3^+(\mathrm{III})=-\mathbf{r}_3+\mathbf{r}_5$	$\begin{pmatrix}\mathbf{a}_1^+(\mathrm{III})\\ \mathbf{a}_2^+(\mathrm{III})\\ \mathbf{a}_3^+(\mathrm{III})\end{pmatrix}=\frac{1}{\tau}\mathsf{M}^2\begin{pmatrix}\mathbf{a}_1(\mathrm{I})\\ \mathbf{a}_2(\mathrm{I})\\ \mathbf{a}_3(\mathrm{I})\end{pmatrix}$
IV:	$\mathbf{a}_1^+(\mathrm{IV})=\mathbf{r}_1-\mathbf{r}_2$ $\mathbf{a}_2^+(\mathrm{IV})=\mathbf{r}_3+\mathbf{r}_6$ $\mathbf{a}_3^+(\mathrm{IV})=-\mathbf{r}_4-\mathbf{r}_5$	$\begin{pmatrix}\mathbf{a}_1^+(\mathrm{IV})\\ \mathbf{a}_2^+(\mathrm{IV})\\ \mathbf{a}_3^+(\mathrm{IV})\end{pmatrix}=\frac{1}{\tau}\mathsf{M}^3\begin{pmatrix}\mathbf{a}_2(\mathrm{I})\\ \mathbf{a}_2(\mathrm{I})\\ \mathbf{a}_3(\mathrm{I})\end{pmatrix}$
V:	$\mathbf{a}_1^+(\mathrm{V})=\mathbf{r}_1-\mathbf{r}_3$ $\mathbf{a}_2^+(\mathrm{V})=\mathbf{r}_2+\mathbf{r}_5$ $\mathbf{a}_3^+(\mathrm{V})=\mathbf{r}_4+\mathbf{r}_6$	$\begin{pmatrix}\mathbf{a}_1^+(\mathrm{V})\\ \mathbf{a}_2^+(\mathrm{V})\\ \mathbf{a}_3^+(\mathrm{V})\end{pmatrix}=\frac{1}{\tau}\mathsf{M}^4\begin{pmatrix}\mathbf{a}_1(\mathrm{I})\\ \mathbf{a}_2(\mathrm{I})\\ \mathbf{a}_3(\mathrm{I})\end{pmatrix}$

where $\mathsf{n}=(n_1, n_2, n_3, n_4, n_5, n_6)$ with n_i equal to zero or positive or negative integers. This relation is valid everywhere in the material. Unfortunately, (3.1) requires as many n's as there are atoms in the material. It may, however, be possible to reduce the number of n's needed with the aid of the reference lattices. In I, the 'unit cell' for the **a** lattice was found to contain 32 atomic sites as listed in Table 6. Here we adopt the choice of $\{\mathbf{a}_i(\mathrm{I})\}$ for the **a** lattice and, consequently, $\{\mathbf{a}_i^+(\mathrm{I})\}$ is chosen for the a^+ basis.

It is intriguing to note that the eight basic atomic positions, numbered 1 to 8 in Table 6, generate the rest of the atomic positions by $\mathbf{a}_i^+$ translations. These eight groups can be further reduced to four since the atomic positions have equivalent positions produced by a translation based on the **a** lattice. Atomic sites 7, 6 and 5 can be replaced by $7'=7+[\bar{1}10]$, $6'=6+[0\bar{1}1]$ and $5'=5+[10\bar{1}]$, respectively. (7, 6 and 5 in Table 6 are therefore replaced by 7', 6' and 5'.) It

Table 6. *The atomic sites in the a cell*

$\{\mathbf{a}_i(\mathrm{I})\}$ and $\{\mathbf{a}_i^+(\mathrm{I})\}$ are used to generate this table.

I	No. 1	(0, 0, 0)	No. 8	$\left(\frac{\tau}{2},\frac{\tau}{2},\frac{\tau}{2}\right)$
	No. 17	No. $1+\mathbf{a}_1^+$	No. 18	No. $8-\mathbf{a}_1^+$
[111]	No. 23	No. $1+\mathbf{a}_2^+$	No. 26	No. $8-\mathbf{a}_2^+$
	No. 29	No. $1+\mathbf{a}_3^+$	No. 28	No. $8-\mathbf{a}_3^+$
II	No. 2	$\left(\frac{\tau-1}{2},\frac{1}{2},0\right)$	No. 7	$\left(\frac{1}{2},\frac{\tau-1}{2},\frac{\tau}{2}\right)$
	No. 21	No. $2-\mathbf{a}_1^+$	No. 25	No. $7+\mathbf{a}_1^+$
[$\bar{1}$11]	No. 15	No. $2+\mathbf{a}_2^+$	No. 19	No. $7-\mathbf{a}_2^+$
	No. 11	No. $2+\mathbf{a}_3^+$	No. 13	No. $7-\mathbf{a}_3^+$
III	No. 3	$\left(0,\frac{\tau-1}{2},\frac{1}{2}\right)$	No. 6	$\left(\frac{\tau}{2},\frac{1}{2},\frac{\tau-1}{2}\right)$
	No. 9	No. $3+\mathbf{a}_1^+$	No. 12	No. $6-\mathbf{a}_1^+$
[1$\bar{1}$1]	No. 30	No. $3-\mathbf{a}_2^+$	No. 32	No. $6+\mathbf{a}_2^+$
	No. 22	No. $3+\mathbf{a}_3^+$	No. 24	No. $6-\mathbf{a}_3^+$
IV	No. 4	$\left(\frac{1}{2},0,\frac{\tau-1}{2}\right)$	No. 5	$\left(\frac{\tau-1}{2},\frac{\tau}{2},\frac{1}{2}\right)$
	No. 27	No. $4+\mathbf{a}_1^+$	No. 31	No. $5-\mathbf{a}_1^+$
[11$\bar{1}$]	No. 10	No. $4+\mathbf{a}_2^+$	No. 14	No. $5-\mathbf{a}_2^+$
	No. 16	No. $4-\mathbf{a}_3^+$	No. 20	No. $5+\mathbf{a}_3^+$

is significant that these reduced groups are aligned along the ⟨111⟩ directions, where these directions are indicated in Table 6.

Each group of eight positions consists of two partial cubes shifted along a ⟨111⟩ direction. These partial cubes are half of the cube whose basis is the $\mathbf{a}_i^+$'s. Before proceeding, we should note that each of the 32 atomic sites returns to one of these positions about 80% of the time when the icosahedral transformation, M, is repeatedly performed. (The missing icosahedral positions are generated shortly.) This property implies that the 32 atomic sites satisfy icosahedral symmetry, but not exhaustively. The eight basic positions, 1 to 8, generate only themselves and others of the 32 positions after repeated transformation. Therefore, an analysis based on any one of the five coordinate systems is equally valid. We will choose $\mathbf{a}_i(\mathrm{I})$ and $\mathbf{a}_i^+(\mathrm{I})$ and drop the use of I, hereafter.

When the four groups of the atomic positions are viewed along their appropriate ⟨111⟩ directions, they appear identical, except for the fact that their origins are located at four different atomic positions. Fig. 2 shows the atomic sites for group I referred to the [111] axis. At this stage, we find additional possible atomic sites: *A*, *B*, *C* and *D* belonging to the a^+ frame originating at site 1, and *a*, *b*, *c* and *d* belonging to the a^+ frame originating at site 8. Along the [111], the distance between site 1 and site *a* is equal to the distance between site 8 and site $(1+\mathbf{a}_1+\mathbf{a}_2+\mathbf{a}_3)=$ site [111]. This distance is $[(2-\tau)/2]\sqrt{3}|\mathbf{a}_i|=(1/2\tau^2)\sqrt{3}|\mathbf{a}_i|$. Site 8 is located at a distance $(\tau/2)\sqrt{3}|\mathbf{a}_i|$ from site 1. According to the reference lattice, site [111] is one of the legitimate atomic sites. Therefore, it is tempting to consider position *a* to be as legitimate

as the [111] site. Similarly, position A can be considered to be legitimate since the distance between site A and site 8 is equal to that between 1 and a. Then let us consider b, c and d and B, C and D. Position d is aligned along the [111] direction with the [001] and [110] lattice sites when joined with site 28. These lattice sites are a distance $[1-(\tau/2)]\sqrt{3}|\mathbf{a}_i|$ from sites d and 28. In the same fashion, the distance between sites 18 and c and sites [100] and [011], respectively, is $[1-(\tau/2)]\sqrt{3}|\boldsymbol{a}_i|$ along the [111] direction. A similar situation holds for sites 26 and b and [101] and [010] along the $[1\bar{1}1]$ direction.

In other words, all the corner positions in the two small cubes of a^+ become possible atomic sites when position a is considered to be a legitimate atomic site. Similarly, when site A is recognized to be legitimate, sites B, C and D can be recognized as positions equivalent to A in the [111] direction to be paired with sites 26, 18 and 28. Thus, all the new sites in the a^+ cubes can be considered as atomic sites, where these positions still satisfy the general rule (3.1).

These sites were not shown in the **a** lattice described in I. For that **a** lattice, space-filling decorated rhombohedra were used, with no sites inside rhombohedra. The sites a and A are vertices along the shortest body diagonal of an imaginary flat ($\alpha = 116.6°$) rhombohedron which is hidden inside the pointed ($\alpha = 63.4°$) rhombohedron. This situation is illustrated in Fig. 3 for the [111] direction.

Similar arrangements can be constructed for the other ⟨111⟩ directions. The possible atomic sites within the complete unit cell are listed in Table 7. It should be noted that the listed positions have translational symmetry with respect to the $\mathbf{a}_i$'s, while $\mathbf{a}_i^+$'s merely give the length of the a^+ cube edges. The four atomic positions, 1, 2, 3 and 4, serve as the origins of four a^+ cubes and each cube creates its companion cube through a shift of $(2-\tau)\sqrt{3}|a_i|/2$ along the appropriate ⟨111⟩ direction. This lattice serves as the reference lattice for this material by providing all the possible atomic sites. An illustration of the new sites along the [111] direction is shown in Fig. 4 on the left. This reference lattice will serve as a guide to all of the possible atomic sites in the icosahedral phase material.

4. The occupancy of atomic sites and staggered layers

There are now 64 possible atomic sites in the unit cell of the reference lattice. Within realistic physical densities, no more than half of these sites can be occupied by atoms. Of course, the occupied sites in one local unit cell may be different from those occupied in another local unit cell. The object of this section is to derive the rule that governs the local atomic occupancy.

An allowed stacking of atomic layers is shown in Fig. 5. In this diagram, sites 1, a, A and 8 can represent layering along a threefold direction. There is no way of knowing *a priori* how to reference a particular atomic layering position. For example, a pointed rhombohedron may start at layer position $A \rightarrow 1$ (Fig. 5*a*) just as well as at position a (Fig. 5*b*). As a result, a permitted sequence of the rhombohedral construction may appear as a staggering of layers where the sequence 1, a, A, 8, ... changes locally to 1, a, 1, a, ...

The occupancy sequence of atomic sites can result in a staggering of layers. To make the situation more complicated, the density limit requires about half of the sites to be vacant. In any event, it is already clear that the actual atomic construction may have little resemblance to the stacking in the unit cell of the reference lattice. The staggered occupancy of layers creates locally interpenetrating rhombohedra as shown in Fig. 4, where a reference lattice is shown on the left and an allowed atomic sequence on the right.

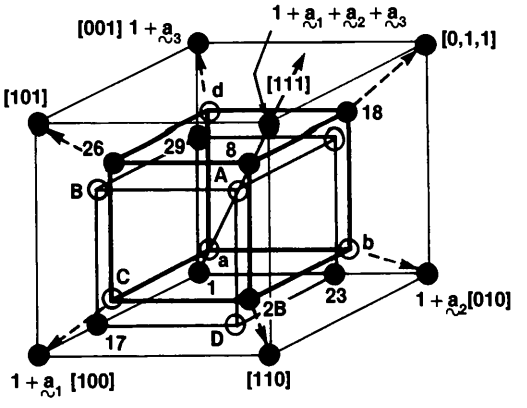

Fig. 2. Atomic sites for group I, showing the locations of additional sites a, b, c, d and A, B, C, D.

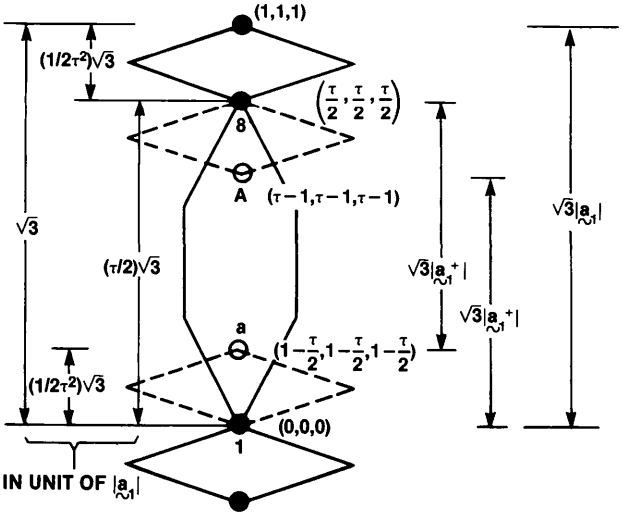

Fig. 3. Location of sites a and A within a pointed rhombohedron, showing imaginary flat rhombohedra.

Table 7. *The atomic sites in the reference unit cell*

I	No. 1	$(0,0,0)$	a_1	No. $1+\xi_I$
	No. 17	No. $1+\mathbf{a}_1^+$	b_1	No. $17+\xi_I$
	No. 23	No. $1+\mathbf{a}_2^+$	c_1	No. $23+\xi_I$
	No. 29	No. $1+\mathbf{a}_3^+$	d_1	No. $29+\xi_I$
	A_1	No. $1+\mathbf{a}_1^++\mathbf{a}_2^++\mathbf{a}_3^+$	No. 8	$A_1+\xi_I$
	B_1	No. $1+\mathbf{a}_1^++\mathbf{a}_3^+$	No. 26	$B_1+\xi_I$
	C_1	No. $1+\mathbf{a}_2^++\mathbf{a}_3^+$	No. 18	$C_1+\xi_I$
	D_1	No. $1+\mathbf{a}_1^++\mathbf{a}_2^+$	No. 28	$D_1+\xi_I$
II	No. 2	$\left(\frac{\tau-1}{2},\frac{1}{2},0\right)$	a_2	No. $2+\xi_{II}$
	No. 21	No. $2-\mathbf{a}_1^+$	b_2	No. $21+\xi_{II}$
	No. 15	No. $2+\mathbf{a}_2^+$	c_2	No. $15+\xi_{II}$
	No. 11	No. $2+\mathbf{a}_3^+$	d_2	No. $11+\xi_{II}$
	A_2	No. $2-\mathbf{a}_1^++\mathbf{a}_2^++\mathbf{a}_3^+$	No. 7′	$A_2+\xi_{II}=$ No. $7+[\bar{1}10]$
	B_2	No. $2+\mathbf{a}_2^++\mathbf{a}_3^+$	No. 25′	$B_2+\xi_{II}=$ No. $25+[\bar{1}10]$
	C_2	No. $2-\mathbf{a}_1^++\mathbf{a}_3^+$	No. 19′	$C_2+\xi_{II}=$ No. $19+[\bar{1}10]$
	D_2	No. $2-\mathbf{a}_1^++\mathbf{a}_2^+$	No. 13′	$D_2+\xi_{II}=$ No. $13+[\bar{1}10]$
III	No. 3	$\left(0,\frac{\tau-1}{2},\frac{1}{2}\right)$	a_3	No. $3+\xi_{III}$
	No. 9	No. $3+\mathbf{a}_1^+$	b_3	No. $9+\xi_{III}$
	No. 30	No. $3-\mathbf{a}_2^+$	c_3	No. $30+\xi_{III}$
	No. 22	No. $3+\mathbf{a}_3^+$	d_3	No. $22+\xi_{III}$
	A_3	No. $3+\mathbf{a}_1^+-\mathbf{a}_2^++\mathbf{a}_3^+$	No. 6′	$A_3+\xi_{III}=$ No. $6+[0\bar{1}1]$
	B_3	No. $3-\mathbf{a}_2^++\mathbf{a}_3^+$	No. 12′	$B_3+\xi_{III}=$ No. $12+[0\bar{1}1]$
	C_3	No. $3+\mathbf{a}_1^++\mathbf{a}_3^+$	No. 32′	$C_3+\xi_{III}=$ No. $32+[0\bar{1}1]$
	D_3	No. $3+\mathbf{a}_1^+-\mathbf{a}_2^+$	No. 24	$D_3+\xi_{III}=$ No. $24+[0\bar{1}1]$
IV	No. 4	$\left(\frac{1}{2},0,\frac{\tau-1}{2}\right)$	a_4	No. $4+\xi_{IV}$
	No. 27	No. $4+\mathbf{a}_1^+$	b_4	No. $27+\xi_{IV}$
	No. 10	No. $4+\mathbf{a}_2^+$	c_4	No. $10+\xi_{IV}$
	No. 16	No. $4-\mathbf{a}_3^+$	d_4	No. $16+\xi_{IV}$
	A_4	No. $4+\mathbf{a}_1^++\mathbf{a}_2^+-\mathbf{a}_3^+$	No. 5′	$A_4+\xi_{IV}=$ No. $5+[10\bar{1}]$
	B_4	No. $4+\mathbf{a}_2^+-\mathbf{a}_3^+$	No. 31′	$B_4+\xi_{IV}=$ No. $31+[10\bar{1}]$
	C_4	No. $4+\mathbf{a}_1^+-\mathbf{a}_3^+$	No. 14′	$C_4+\xi_{IV}=$ No. $14+[10\bar{1}]$
	D_4	No. $4+\mathbf{a}_1^++\mathbf{a}_2^+$	No. 20′	$D_4+\xi_{IV}=$ No. $20+[10\bar{1}]$

$$\xi_I=\left[1-\frac{\tau}{2},1-\frac{\tau}{2},1-\frac{\tau}{2}\right],$$

$$\xi_{II}=\left[-\left(1-\frac{\tau}{2}\right),1-\frac{\tau}{2},1-\frac{\tau}{2}\right],$$

$$\xi_{III}=\left[1-\frac{\tau}{2},-\left(1-\frac{\tau}{2}\right),1-\frac{\tau}{2}\right],$$

$$\xi_{IV}=\left[1-\frac{\tau}{2},1-\frac{\tau}{2},-\left(1-\frac{\tau}{2}\right),\right]$$

Usually, local nonperiodic effects are accommodated into the description of a structure using the concept of incommensurate modulations on a reference lattice. There, the modulation periodicity is generally greater than that of the unit cell. In our case, the construction using interpenetrating rhombohedra requires modulations with periodicities shorter than that of the unit cell – *i.e.* internal modulations rather than the external modulations usually accepted in modulated crystals.

We introduce here the appearance of diffraction modulations involving Umklapp processes (Reiter & Moss, 1982). Suppose the unit cell of the reference lattice has a lattice constant a, and the periodicity of

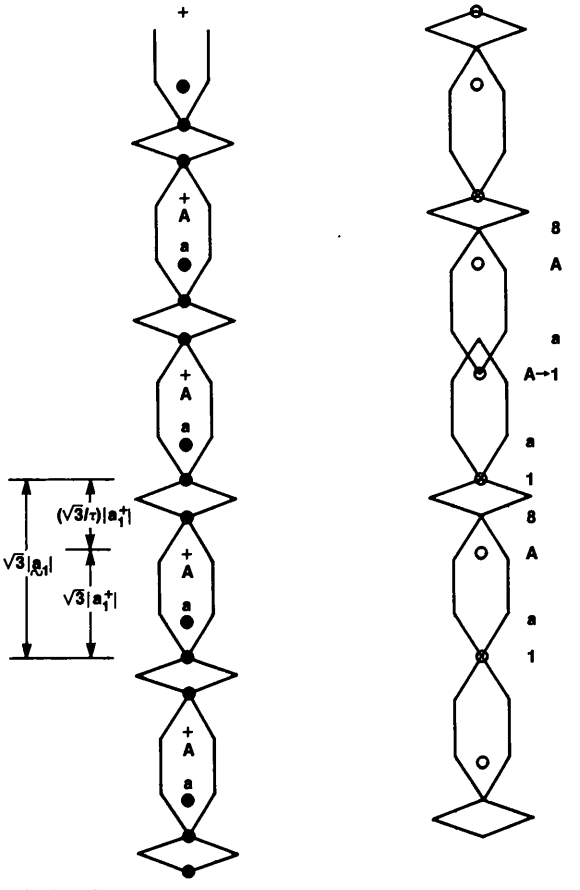

Fig. 4. A reference lattice sequence on the left and an allowed atomic occupancy sequence on the right.

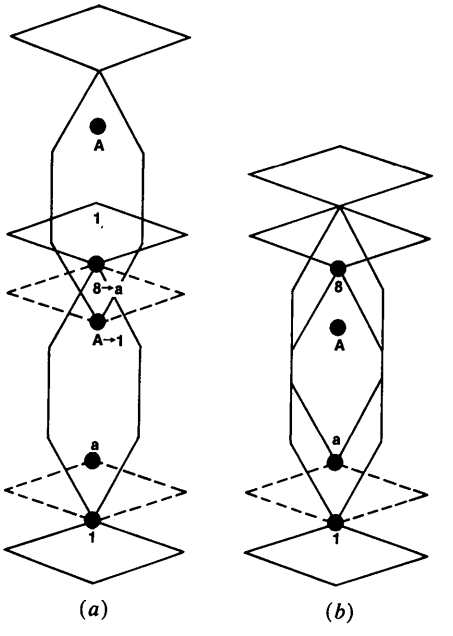

Fig. 5. Possible stacking sequence along a ⟨111⟩ direction. (*a*) A pointed rhombohedron starts at site *A*. (*b*) A pointed rhombohedron starts at site *a*.

the internal modulation is given by $a/(H+\varepsilon)$, where H is an integer and ε is an irrational number smaller than one. In the geometrical structure factor, this will provide the fundamental mode of modulations, $\Delta q=(H+\varepsilon)/a$, which results in the total phase, $(q+n\Delta q)a=qa+n(H+\varepsilon)$. Since q is the momentum transfer caused by the reference lattice, qa is an integer. Thus, the total phase is given by an integer $+$ $n\varepsilon$. This is an Umklapp process of the fundamental mode of modulations, $\Delta q'=\varepsilon/a$; *i.e.* the fundamental mode is the external modulation, whose periodicity is a/ε, which is larger than a.

Based on this concept, we attempt to understand the staggered occupancy of sites in this structure in terms of the stacking rule of layers over a long range. As shown in Fig. 5, the staggering causes a shift equal to the length of the shortest body diagonal of the flat rhombohedron, $(2-\tau)/2=(1/2\tau^2)$ in units of $\sqrt{3}|\mathbf{a}_i|$, where a pointed rhombohedron takes over. The longest body diagonal of the pointed rhombohedron is equal to $(\tau/2)$ in the same units, and the ratio of these two lengths is $\tau^3=2\tau+1$. Therefore, the internal modulation due to staggering must involve either τ^2, τ^3, or maybe both. We observe that the lattice constant of the reference lattice is written

$$|\mathbf{a}_i|=|\mathbf{a}_i^+|+(1/\tau)|\mathbf{a}_i^+|,$$

where the last term is also twice the staggering (shift) distance projected back to the ⟨100⟩ direction. Therefore, we can now view the staggering as the result of the long-range occupancy sequence of either the layers or of the a^+ and the (a^+/τ) cubes.

The experimental results in I showed that there are two sets of modulations in momentum space, one of which, after conversion into real space, was considered as atomic correlation distances leading to the creation of the reference lattice. The second set of six modulations derived from the experimental data was about 4.2 times larger (in momentum space) than the first set. Since the experimental error in electron diffraction is large, the ratio of these magnitudes should be understood to be $2\tau+1=\tau^3(=4.236\ldots)$ in actuality. This second set of modulations, which is considered to be the fundamental modulation (*e.g.* Bancel, Heiney, Stephens, Goldman & Horn, 1985), cannot be referred to correlations because the distances are unrealistically small (*i.e.* of order 0.1 nm). We consider that this set is related to the staggering of the layer occupancy sequence, as revealed by the internal modulations, $|\mathbf{q}^{(2)}|=\tau^3|\mathbf{q}^{(1)}|$. From the foregoing, $\mathbf{a}_i$ and $\mathbf{a}_i^+$ are inversely proportional to $|\mathbf{q}^{(1)}|$, and the periodicity of the internal modulation (in real space) is $(1/\tau^3)$ times $\mathbf{a}_i$ or $\mathbf{a}_i^+$. This is equivalent, *via* an Umklapp process, to $1/(\tau^3-4)$, where 4 is the integer closest to τ^3. Since

$$\tau^3-\tau^{-3}=4, \tag{4.1}$$

the external modulation periodicity is given by $\tau^3\mathbf{a}_i$.

As suggested above, this modulation periodicity can be viewed as the unit of the stacking occupation sequence modifying the reference lattice. This can be achieved using a sequence of a_i^+ and $(1/\tau)a_i^+$ cubes as shown, for example, in Fig. 4 on the right. The length $\tau^3|\mathbf{a}_i|$ corresponds to five a_i^+ plus three $(1/\tau)a_i^+$ cubes:

$$5|\mathbf{a}_i^+|+3(1/\tau)|\mathbf{a}_i^+|=\{5(1/\tau)+3(1/\tau^2)\}|\mathbf{a}_i| =\tau^3|\mathbf{a}_i|. \tag{4.2}$$

It appears as if the above analysis leads to the conclusion that the structure can be represented by a reference lattice with modulation period $\tau^3|\mathbf{a}_i|$, within which five a_i^+ cubes and three $(1/\tau)a_i^+$ cubes should be found. Atoms are expected to occupy approximately one site out of every two as shown on the right side of Fig. 4. Even though the external modulation periodicity was found, the sequence of a_i^+ and $(1/\tau)a_i^+$ cubes within this periodicity was not given. The modulation periodicity is very suggestive that the sequence of the two types of cubes is a Fibonacci sequence, but our conclusion so far only requires an incommensurate periodic modulation over the reference lattice. Since Fibonacci sequences are nonperiodic, a structure with periodic modulations could not indefinitely follow a Fibonacci sequence rule. The appearance of a partial Fibonacci sequence, however, suggests that the above arguments can be generalized.

5. A general method for the determination of staggering stacking sequences

Let N and L be an integer and a Lucas number, respectively. The following relation then holds:

$$\tau^N+(-1)^N\tau^{-N}=L. \tag{5.1}$$

This relation was used in the previous section, with $N=3$ and $L=4$. If the staggered stacking occupancy sequence is a nonperiodic Fibonacci sequence composed of a^+ cubes (τ^{-1}), and $(1/\tau)a^+$ cubes (τ^{-2}), a partial sequence that involves the total number of the cubes equal to a Fibonacci number always has the total length $\tau^N|\mathbf{a}_i|$. Examples are shown in the following, where A and B represent the a^+ cube and $(1/\tau)a^+$ cube, respectively:

τ^0: AB (5.2.1)

τ^1: ABA (5.2.2)

τ^2: $ABAAB$ (5.2.3)

τ^3: $ABAABABA$ (5.2.4)

τ^4: $ABAABABAABAAB$ (5.2.5)

$$\vdots$$

τ^N: $\underbrace{(AB\ldots}_{\text{Sequence } \tau^{N-1}}\underbrace{)(AB\ldots}_{\text{Sequence } \tau^{N-2}}).$ (5.2.6)

These sequences are classified by the total length τ^N in the unit-cell length $|\mathbf{a}_i|$. One can immediately see that if any of these sequences exists in the real structure as an external modulation, the internal modulation τ^{-N} will appear in the diffraction patterns.

If we compare a τ^N sequence containing 144 atoms with a periodic assembly of the τ^3 sequence of the same size, the difference in the diffraction patterns is a shift of the diffraction peaks and slight changes in the peak intensities. The differences are so subtle that the patterns are almost identical. The periodic assembly of sequences (a modulated crystal) cannot be distinguished from a nonperiodic material.

This situation implies that the true nonperiodic sequence could be approximated by a periodic assembly of the subsequences and better by the sum of those assemblies with different periodicities denoted by M:

$$\tau^N \text{ sequence} = \sum_{M<N} (\tau^M \text{ sequence})(\tau^M \text{ sequence}) \ldots (\tau^M \text{ sequence}). \quad (5.3)$$

This is analogous to a transition from the Fourier series to the Fourier integral. Physically, this is equivalent to the view that the icosahedral material is composed of many periodic crystals *coexisting everywhere*, which would be inconsistent with microdomain models. In diffraction, the model always displays a set of internal modulations, τ^{-M}, as a result of the external modulations τ^M, because of (5.1).

Each of these external modulations will only show that the subsequences, M, are composed of the appropriate number of a^+ and $(1/\tau)a^+$ cubes. When taken together, they yield information on the arrangement of sequences of A and B, *i.e.* the staggering sequence of the a^+ and $(1/\tau)a^+$ cubes can be derived. To complete a perfect sequence of τ^N, we require all of the modulations up to τ^N (or τ^{-N}). Of course, this is not experimentally possible, because the scattering angles are limited and the precision is not infinite.

The preceding argument can be generalized in the following way. Let $f(n)$ be a function of atomic site n representing the occupancy and staggered stacking at n. The atomic scattering factors in the X-ray (electron) structure factor will be multiplied by this function. This function can be written as a sum of periodic functions, $g^{(i)}$, whose periodicities are arbitrarily chosen to be $L^{(i)}$:

$$f(n) = \sum_i g^{(i)}(n). \quad (5.4)$$

Since $g^{(i)}(n)$ can be written in terms of a Fourier series whose fundamental mode is $(1/L^{(i)})$, we obtain

$$f(n) = \sum_i \sum_{m_i} \hat{g}^{(i)}_{(m_i)} \sin(2\pi m_i n / L^{(i)}). \quad (5.5)$$

The unusual structure factor resulting from the application of this $f(n)$ requires a calculation over ever-increasing finite domains. The Umklapp process of these fundamental modes will appear as the internal modulation. In particular, when $L^{(i)}$ is a Fibonacci number, the Umklapp process is *uniquely* determined for each fundamental mode. Once these internal modulations are identified by the periodic repetition of sets of patterns within the diffraction patterns, we obtain information on the maximum number for i by counting how many possible sets of repetitions exist and on the $g^{(i)}$ from intensity measurements.

Now back to our model. The above discussion helps determine the actual occupancy sequence of layers within the τ^3 sequence. One can recognize, for example, in the twofold pattern (Fig. 1) the square frames corresponding to $\tau^3|\boldsymbol{b}_i|$, $\tau^2|\mathbf{b}_i|$ and $\tau|\mathbf{b}_i|$, where $\mathbf{b}_i$'s are the reciprocal-lattice vectors for the reference lattice. Therefore, the τ^3 sequence obtained in the previous section is not the only representation of the staggered stacking sequence, and there are the τ^2 and τ sequences within the τ^3 sequence. Consequently, we can conclude that the actual stacking through the a^+ and $(1/\tau)a^+$ cubes is, indeed, the Fibonacci sequence shown in (5.2.4). Because of the lack of information concerning the τ^4, τ^5 *etc.* in the diffraction patterns, we cannot guarantee that the actual sequence follows the Fibonacci sequence indefinitely. In any event, the staggered occupancy sequence derived for layering along one ⟨111⟩ axis, which may be a perfect Fibonacci sequence, will be observed along all four of these axes.

6. Discussion

The derivation of a full atomic scale structure for an icosahedral phase alloy began with I in which the structure of a reference lattice unit cell was derived. In that model, the pattern of atomic sites arose when the rhombohedra were decorated by atomic sites which follow the atomic arrangement rule derived from the experimental data. These decorated rhombohedra, however, were space filling and an isotropic 1-to-1 (flat to pointed) rhombohedral packing was the result.

In II, the possible atomic sites in this unit cell were used, in turn, to derive additional icosahedral atomic positions in the unit cell of the reference lattice. The identification of these positions led to another length scale through the a^+ cube, where the edge ratio between the a unit cell and the a^+ cube is $\tau:1$. It was recognized that the length of the a unit cell is composed of the length of the a^+ cube and that of the $(1/\tau)a^+$ cube, and that the possible atomic positions are given by the total length of the sequence of the a^+ cubes and the $(1/\tau)a^+$ cubes. In this case, the interpenetration of rhombohedra along ⟨111⟩ is real. The occupancy of the atomic sites depends on the sequences of these cubes, thus creating local devi-

ations from periodicity everywhere in the material. These deviations appear in the diffraction patterns as internal modulations. The internal modulations are then connected uniquely (in the present case) to the external modulations through Umklapp processes.

The rules for the occupancy of the atomic sites are thus found through the sequences of atomic layering over a large spatial range. One of these modulation periodicities agrees well with the second set of observed modulations. The appearance of this periodicity is suggestive that the limit of the occupancy sequences should be taken for successively larger periodic modulations. This generalization determines the entire sequence throughout the material (consistent with what can be seen from the experiment).

It is significant that the atomic scale models constructed *via* experimental analysis lead to periodic (modulated) structures rather than aperiodic ones. However, the fact that successively larger periodic arrays are required to complete the description of the occupancy function suggests that the true structure is at the limit of the periodic approximations. This view yields some physical insight into the meaning of almost periodic functions as applied to the Al-Mn icosahedral phase. The unusual form of the structure factor (occupancy function) calculation relevant to the model developed in this series of papers closely resembles the Fourier transform associated with almost periodic functions. This analysis, which was built up of periodic (modulated) sequence models can be used to help define the relationship between classical three-dimensional periodicity and almost (or 'quasi') periodicity in a physical system.

As the physical model is built up along the ⟨111⟩ axes according to the derived occupancy rules, it is possible that long-range flaws may occur. Such flaws would disrupt the perfect Fibonacci sequence while being consistent with the short-range requirements such as the rule that A may have as a neighbor either A or B, but B may only have A as a neighbor. Of course, such flaws would be very difficult to detect experimentally for reasons related to the difficulty of separating periodic and almost periodic lattices.

Viewed thus, the icosahedral phase belongs firmly under the classification of crystal rather than glass. Only in so far as icosahedral packing is relevant to many glasses (and this is considerable), does this structure tell us something new about glasses.

The clue to the discovery of the relationship between the reference lattice we derived and the Fibonacci sequence lay in the fact that two colinear sets of six modulations were derived from the electron diffraction patterns, and the ratio of their magnitudes was close to τ^3. In this regard, it is interesting that it was suggested by Mackay (1976) that a three-dimensional icosahedral construction be attempted based on $\tau^3 - \tau^{-3} = 4$. Similarly, Mackay (1982) noted that inflation of the three-dimensional model results in a coincidence of every other point, while in this paper we suggest that the construction requires that only half of the sites are occupied according to the derived occupancy sequence rule.

References

BANCEL, P. A., HEINEY, P. A., STEPHENS, P. W., GOLDMAN, A. I. & HORN, P. M. (1985). *Phys. Rev. Lett.* **54**, 2422-2425.
KURIYAMA, M., LONG, G. G. & BENDERSKY, L. (1985). *Phys. Rev. Lett.* **55**, 849-851.
LONG, G. G. & KURIYAMA, M. (1986). *Acta Cryst.* A**42**, 156-164.
MACKAY, A. L. (1976). *Phys. Bull.* pp. 495-497.
MACKAY, A. L. (1982). *Physica (Utrecht)*, **114**A, 609-613.
NELSON, D. R. & SACHDEV, S. (1985). *Phys. Rev. B*, **32**, 689-695.
REITER, G. & MOSS, S. C. (1982). *Phys. Rev. B*, **26**, 3520-3522.

Acta Cryst. (1986). A**42**, 172-178

Automated Calculation of Coordinate Transformations for the Superposition of Protein Structures

BY RICHARD B. HONZATKO

Department of Biochemistry and Biophysics, Iowa State University, Ames, Iowa 50011, *USA*

(*Received* 22 *April* 1985; *accepted* 22 *November* 1985)

Abstract

A computer program is described that performs a superposition of two protein structures. The program calculates a coordinate transformation that minimizes the root-mean-square deviation between atoms representing homologous structure in the two proteins. All atoms of the main chain and those atoms of side chains that bear common labels contribute to the calculation of the transformation. Required input by the user is either a small set of integers representing the sequence numbers of spatially equivalent residues in the two proteins and/or the initial and terminal residues of homologous elements of secondary struc-

0108-7673/86/030172-07$01.50